

Kondo Effect in Multiple-Dot Systems

Rui Sakano and Norio Kawakami
Department of Applied Physics, Osaka University,
Suita, Osaka 565-0871, Japan

(Dated: March 23, 2024)

We study the Kondo effect in multiple-dot systems for which the inter- as well as intra-dot Coulomb repulsions are strong, and the inter-dot tunneling is small. The application of the Ward-Takahashi identity to the inter-dot dynamical susceptibility enables us to analytically calculate the conductance for a double-dot system by using the Bethe-ansatz exact solution of the SU(4) impurity Anderson model. It is clarified how the inter-dot Kondo effect enhances or suppresses the conductance under the control of the gate voltage and the magnetic field. We then extend our analysis to multiple-dot systems including more than two dots, and discuss their characteristic transport properties by taking a triple-dot system as an example.

PACS numbers: 68.65.Hb, 71.27.+a, 72.15.Qm, 75.20.Hr

I. INTRODUCTION

Recent advances in semiconductor processing have made it possible to fabricate various nanoscale materials with tunable quantum parameters, revealing various aspects of quantum mechanics. Quantum dot [1, 2] is one of the interesting nanoscale materials. In particular, a lot of works on the Kondo effect in single quantum dot systems have been done both theoretically and experimentally [3, 4, 5, 6, 7, 8, 9, 10, 11, 12]. More recently, double-dot systems or systems with more than two dots have been investigated [13, 14, 15]. In this connection, the Kondo effect in double-dot systems have been studied intensively [16, 17, 18, 19, 20, 21].

Most of the previous studies on multiple-dot systems have treated the intra-dot Coulomb repulsion but have ignored the Coulomb repulsion between quantum dots (inter-dot Coulomb repulsion). We especially focus on the effect of the inter-dot Coulomb repulsion here [22, 23, 24] and study how such electron correlations affect transport properties. Recently, Borda et al. have investigated properties of the Kondo effect in such double-dot systems with a magnetic field by the numerical renormalization group method [24], which may explain the Kondo effect observed experimentally by Wilhelm et al. in a double-dot system [22]. A remarkable point in the above double-dot systems with inter-dot Coulomb repulsion is that enhanced charge fluctuations between the quantum dots induce the "inter-dot Kondo effect", which plays an important role to determine transport properties of the systems. Since the inter-dot Kondo effect is caused not by spin fluctuations but by charge fluctuations between two dots, its influence appears significantly when the dots are connected in series. In particular, by changing the gate voltage or the magnetic field, one can control the conductance via the inter-dot Kondo effect.

In this paper, we investigate transport properties of the double-dot systems with strong intra- and inter-dot Coulomb repulsions mentioned above. We exploit a novel method to treat the Kondo effect at absolute zero: the

application of the Ward-Takahashi identity enables us to use the Bethe-ansatz exact solution of the SU(4) impurity Anderson model to our double-dot system. Our calculation clearly shows that the inter-dot Kondo effect plays an important role on transport, which can be controlled by the gate voltage and the magnetic field. Our method is also applicable to multiple-dot systems including more than two dots. We explore the Kondo effect in such dot systems by taking a triple-dot system as an example.

This paper is organized as follows. In section II, we introduce the model Hamiltonian and outline the method to treat our double-dot system: how the Bethe-ansatz exact solution can be used to compute the conductance at absolute zero. In section III we discuss the results for the conductance with particular emphasis on the gate-voltage control and the magnetic-field control. In section IV we extend our method to a triple-dot system, and discuss its transport properties on the basis of the exact solution. We also mention how we can treat generalized multiple-dot systems including more dots. A brief summary is given in section V.

II. MODEL AND METHOD

We describe our model and method by taking a double-dot system connected in series, which was proposed by Borda et al. [24]. The setup is schematically shown in FIG. 1, where not only the ordinary Coulomb repulsion U , which works inside each dot, but also U^0 between the dots are introduced. We assume that the inter-dot tunneling t is small and the gate voltages are such that the lowest-lying charged states are restricted to the configurations of singly-occupied states, $(n_R; n_L) = (1; 0)$ and $(0; 1)$, where $n_{R(L)}$ is the number of extra electrons on the right (left) dot. This situation is realized in the condition,

$$\mathbb{E}(1; 0) \lesssim \mathbb{E}(0; 1) \lesssim U; U^0 \quad (1)$$

where $E(n_R; n_L)$ is the energy level in the dots measured from the common chemical potential of the two leads. The states $(1;0)$ and $(0;1)$ have a spin $S = 1/2$, associated with the extra electron on the double dots. Then at energies below the charging energy of the double dots, dynamics of the double dots is restricted to the subspace with the 4 possible configurations of $fS_z = 1/2$; $n_R - n_L = 1$ in addition to the unoccupied state of $n_R = n_L = 0$.

The above double-dot system, in which both of intra- and inter-dot Coulomb repulsions are sufficiently strong, may be modeled by the highly correlated degenerate Anderson Hamiltonian H_A ($U; U^0; 1$) supplemented by a inter-dot tunneling term H_T ,

$$H_A = \sum_{\mathbf{x}} \sum_{\sigma} c_{\mathbf{x}\sigma}^\dagger c_{\mathbf{x}\sigma} + \frac{1}{i} \frac{\partial}{\partial x} c_{\mathbf{x}\sigma} + \sum_{\mathbf{x}} \sum_{\sigma} \epsilon_{\mathbf{x}} c_{\mathbf{x}\sigma}^\dagger c_{\mathbf{x}\sigma} + \sum_{\mathbf{x}} \sum_{\sigma} \epsilon_{\mathbf{x}} c_{\mathbf{x}\sigma}^\dagger c_{\mathbf{x}\sigma} + \sum_{\mathbf{x}} \sum_{\sigma} \epsilon_{\mathbf{x}} c_{\mathbf{x}\sigma}^\dagger c_{\mathbf{x}\sigma} + \sum_{\mathbf{x}} \sum_{\sigma} \epsilon_{\mathbf{x}} c_{\mathbf{x}\sigma}^\dagger c_{\mathbf{x}\sigma} \quad (2)$$

$$H_T = t \sum_{\mathbf{x}} c_{\mathbf{x}\sigma}^\dagger c_{\mathbf{x}\sigma} \quad (3)$$

where $c_{\mathbf{x}\sigma}^\dagger$ ($c_{\mathbf{x}\sigma}$) creates (annihilates) a conduction electron at a position \mathbf{x} with spin σ ($\sigma = 1/2$) and orbital index \mathbf{x} . Here we have represented conduction electrons in the leads in the low-energy continuum limit by assuming that its density of states is constant, $\rho = 1/2$. Also we have introduced the orbital index $\mathbf{x} = 1/2$ ($-1/2$) to specify an electron occupying the left (right) lead, which is also used to label the left (right) dot. A state j in the double dots located at $\mathbf{x} = 0$ denotes a singly occupied state and j_i denotes an unoccupied state.

We will discuss transport properties of the system under the gate-voltage control or the magnetic field control. It is thus convenient to write down each energy level ϵ_d as,

$$\epsilon_d = \epsilon + E_C + E_Z; \quad (4)$$

where E_C (E_Z) is the energy difference between the two dots (Zeeman energy). Note that the system possesses SU(4) symmetry with respect to spin and orbital degrees of freedom at $E = E_Z = 0$.

We note here that the Bethe-ansatz exact solution can be obtained for the above four-component Anderson

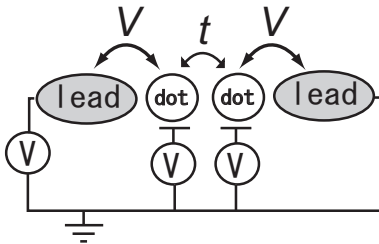


FIG. 1: Schematics of our double-dot system: two dots are connected via tunneling t , and each dot is connected to a lead via V .

Hamiltonian H_A [25], which is referred to as the SU(4) Anderson model henceforth. However, this method allows us to calculate only static quantities, so that we cannot apply the exact solution to transport quantities straightforwardly. In the following, we outline how we can overcome this difficulty to calculate the conductance.

Let us begin with the expression for the conductance in the above double-dot system connected in series, which is obtained in the second order in the tunneling Hamiltonian H_T between two dots,

$$G = \frac{2e^2}{h} \lim_{\omega \rightarrow 0} \frac{\text{Im} \chi_{\text{ops}}(\omega)}{\omega}; \quad (5)$$

where $\chi_{\text{ops}}(\omega)$ is the analytic continuation ($i\eta \rightarrow \omega + i0$) of the dynamical "orbital pseudo-spin" susceptibility for the SU(4) Anderson Hamiltonian H_A (without H_T),

$$\chi_{\text{ops}}(i\eta) = \sum_0^Z d \epsilon^{i\eta} \langle T \hat{T}_z (|\mathbf{f}\rangle(0)) \rangle; \quad (6)$$

with the time-ordering operator T . The corresponding SU(2) operators are defined as

$$\hat{T}_z = \frac{1}{2} (n_R - n_L); \quad \hat{T} = \sum_{\mathbf{x}} j_{\mathbf{x}} \quad (7)$$

These orbital pseudo-spin operators properly describe inter-dot charge fluctuations. As defined above, the eigenvalue $\mathbf{x} = 1/2$ of \hat{T}_z specifies which dot an electron occupies. Eq.(5) means that the low-frequency inter-dot "orbital" susceptibility is essential to determine the conductance.

Although the low-frequency susceptibility is difficult to calculate in general, we can make use of sophisticated techniques developed in the study of the NMR relaxation rate in dilute magnetic alloys [26, 27]: the exact Ward-Takahashi relation for the low-frequency dynamical pseudo-spin susceptibility is obtained, at zero temperature, as

$$\lim_{\omega \rightarrow 0} \frac{\text{Im} \chi_{\text{ops}}(\omega)}{\omega} = \sum_{\mathbf{x}} \sum_{\mathbf{y}} (\Gamma_{\mathbf{x}})^2 \rho_{\mathbf{y}}; \quad (8)$$

with

$$K_{\mathbf{d}} = \begin{cases} \frac{h}{d} & \text{for } \mathbf{d} \neq \mathbf{d}_0 \\ \frac{h}{d} + \frac{d_0}{d} & \text{for } \mathbf{d} = \mathbf{d}_0 \end{cases} \quad (9)$$

where $\rho_{\mathbf{d}}(\epsilon_{\mathbf{d}})$ is the density of states (self energy) for an electron at the Fermi level in the dot \mathbf{d} .

We note that the second line of Eq.(9) is the well-known Korringa relation [26] in the context of NMR relaxation theory, and the first line is its extension to the case having a finite energy-level splitting [27]. Since the static susceptibility can be calculated by the exact solution, we need to evaluate the density of states $\rho_{\mathbf{d}}$ and the self

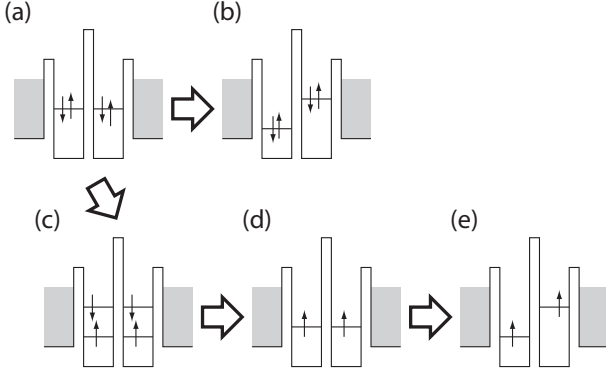


FIG. 2: Schematic description of the energy states in the double dots connected in series: (a) SU(4) symmetric case, (b) asymmetric case, (c) symmetric case in a magnetic field, (d) symmetric case in a strong magnetic field, (e) asymmetric case in a strong magnetic field.

energy ϵ_d . Fortunately, this can be done by exploiting the Friedel sum rule. First recall that the phase shift of an electron in the double dots at the Fermi level is obtained from the average number of electrons n_d in the double dots: $\phi = n_d \pi$ (Friedel sum rule). Then, the density of states and the selfenergy at the Fermi level is given by

$$\rho_d = \frac{\sin^2 \phi}{\pi}; \quad (10)$$

$$\epsilon_d = \epsilon_0 + \cot \phi \quad (11)$$

with the resonance width Γ due to the mixing V . Note that the electron number n_d can be evaluated by the exact solution.

Combining all the above relations, we can compute the conductance at zero temperature: the quantities in the right hand side of Eq.(9), ρ_d , ϵ_d , $\chi_{\text{ops}}(0)$, can be evaluated by means of the Bethe-ansatz solution of the SU(4) Anderson model [25].

III. DOUBLE-DOT SYSTEM

We study the conductance in several cases in our double-dot system, which are schematically shown in FIG. 2.

A. Charge fluctuations in symmetric double dots

Let us start with the double-dot system shown in FIG. 2(a), where the energy levels of two dots are same, which we refer to as the symmetric dots in this paper: there are 4 degenerate electron states including spin degrees of freedom. In this case, from the expressions (5), (8) and (9) we write down the conductance in the absence of the

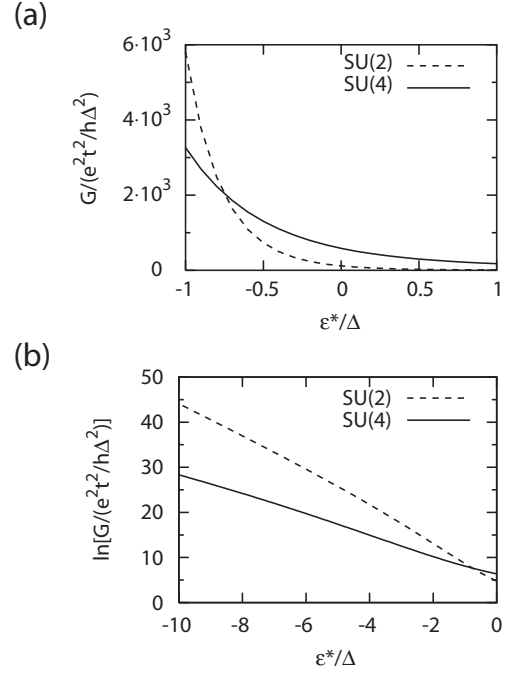


FIG. 3: (a) Conductance in the cases of the SU(4) and SU(2) symmetric double-dot systems as a function of the renormalized energy level ϵ^* . (b) conductance on log scale: we can see distinct exponential dependence between the SU(4) (zero field) and SU(2) (strong field) cases in the Kondo regime.

magnetic field as,

$$G = 2^2 \frac{e^2}{h} t^2 \chi_{\text{ops}}(0)^2$$

$$= 4^2 \frac{e^2}{h} t^2 \chi_{\text{ops}}(0)^2 : \quad (12)$$

By computing static pseudo-spin susceptibility $\chi_{\text{ops}}(0)$ by means of the Bethe-ansatz solution of the SU(4) Anderson model, we evaluate the conductance as a function of the effective energy level ϵ^* [28]. The results are shown in FIG. 3. When the dot-level ϵ is above the Fermi level, the conductance is small, since the resonant tunneling does not occur. As ϵ goes down through the Fermi level, the conductance is enhanced by the Kondo effect, which is analogous to an ordinary single dot case. However, in contrast to the single dot system, for which the conductance is saturated in the Kondo limit with deep ϵ , it continues to increase exponentially. The increase is caused by the inter-dot charge fluctuations enhanced by the inter-dot "orbital" Kondo effect [22, 23, 24]. Since the static susceptibility $\chi_{\text{ops}}(0)$ is inversely proportional to the Kondo temperature $T_K \propto \exp(-\epsilon^*)$, the conductance has the exponential dependence like $\exp(-2\epsilon^*)$.

Note that the ordinary spin Kondo effect and the inter-dot Kondo effect both emerge in the above SU(4) symmetric case. Therefore, in order to see the above characteristic enhancement of the conductance more clearly, we consider an extreme case with strong magnetic fields,

where the spin Kondo effect is completely suppressed. Shown in FIG. 3(b) is the conductance in strong magnetic fields (corresponding to FIG. 2(d)). We can see the enhancement of the conductance due to inter-dot Kondo effect with SU(2) symmetry. In this case, the corresponding Kondo temperature is given by $T_K \propto \exp(-2\beta)$, so that the increase of the conductance, $\propto \exp(4\beta)$, is more significant in comparison with the zero field case. These results are indeed seen in log-scale plots given in FIG. 3, which clearly features the exponential dependence of the conductance in the Kondo regime.

B. Symmetric double dots: magnetic-field control

It is seen from FIG. 3 that in the Kondo regime with deep dot levels, the conductance in the SU(2) case (strong field) is larger than that in the SU(4) case (zero field). This implies that the conductance may be monotonically enhanced in the presence of a magnetic field. To clarify this point, we focus on the field-dependence of the conductance for the SU(4) symmetric double-dot system (shown in FIG. 2(c)) in the Kondo regime. Following the way outlined above, we can derive the conductance in this case,

$$G = 2^2 \frac{e^2}{h} t^2 \frac{\hbar}{h} \chi_{\text{ops}}^2(0) + \chi_{\text{ops}}^2(0) : \quad (13)$$

By exploiting the exact solution of the SU(4) Anderson model in the Kondo regime (so-called Coqblin-Schrieffer model), we compute the conductance as a function of the Zeeman splitting E_Z , which is shown in FIG. 4. Also, the effective Kondo temperature $T_K(E_Z)$ is plotted as a function of the Zeeman splitting on the log-log scale in FIG. 5. Here we assume that the direction of the magnetic field is parallel to spin. It is seen that the magnetic fields enhance the conductance, in contrast to the ordinary Kondo effect in a single-dot system. The inter-dot Kondo effect is caused by the degenerate energy levels in two dots, which still possess SU(2) symmetry in strong magnetic fields. Since the pseudo-spin susceptibility $\chi_{\text{ops}}(0)$ increases with the increase of the field, thus resulting in the enhanced conductance. In strong fields, the effective Kondo temperature, which is defined by the inverse of $\chi_{\text{ops}}(0)$, is given by [25],

$$T_K(E_Z) = T_K(0) (E_Z = T_K(0))^{-1}; \quad (14)$$

so that the conductance increases as

$$G \propto (T_K(E_Z) = T_K(0))^{-2} (E_Z = T_K(0))^2 : \quad (15)$$

Here we note that the conductance for electrons with spin parallel (anti-parallel) to the magnetic field increases (decreases). This effect might be utilized for spin-current control by using double-dot systems. The above results agree with those of Borda et al. obtained by the numerical renormalization group analysis [24].

It is to be noted here that the SU(4) Kondo resonance has been observed not only in a double-dot system [22] but also in a single vertical quantum dot whose symmetric shape gives rise to SU(4) internal degrees of freedom [29]. Also, STM experiments on a Cr(001) surface have found the SU(4) Kondo resonance, where the degeneracy of d_{xz} and d_{yz} states gives the additional orbital degrees of freedom [30]. Our results are also consistent with these findings.

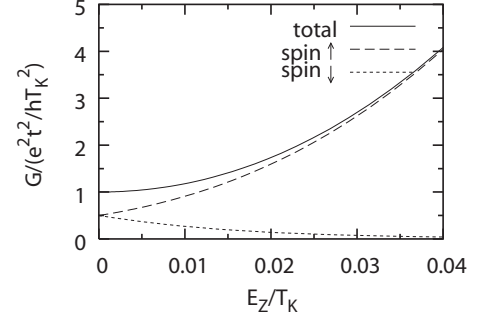


FIG. 4: Conductance as a function of the Zeeman splitting in the Kondo regime. We also show the contribution of the electrons with spins parallel (anti-parallel) to the magnetic field. Note that $T_K = T_K(E_Z = 0)$ is the Kondo temperature of the SU(4) Anderson model.

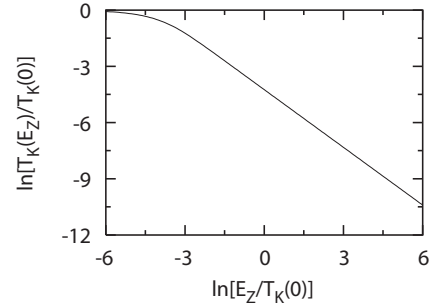


FIG. 5: The effective Kondo temperature as a function of the Zeeman splitting on log-log scale.

C. A symmetric double dots: gate-voltage control

Next, we consider how the conductance is influenced by the energy-level difference between the two dots, which is controlled by changing the gate voltage of each dot. We study two typical cases in the Kondo regime: zero magnetic field (FIG. 2(b)) and strong magnetic fields (FIG. 2(e)).

From the expressions (5) and (8)–(11), the conductance at zero field is written as

$$G = 4 \frac{e^2}{h} t^2 \frac{\sin^2(\frac{\ln_L i}{E^2} - \frac{\ln_R i}{E^2})}{E^2} : \quad (16)$$

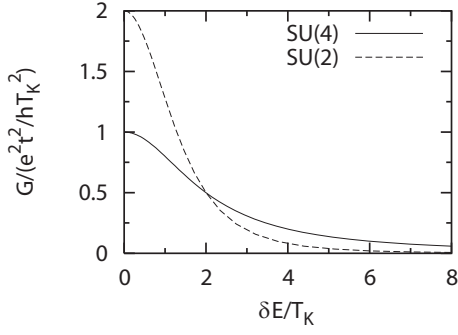


FIG. 6: Conductance as a function of the energy difference E between two dots. We take $T_K = T_K(E_z = 0)$ for the SU(4) double-dot case (zero field) and $T_K = T_K(E_z = 1)$ for the SU(2) double-dot case (strong field).

We compute the conductance as a function of energy differences E . We also study the conductance in strong magnetic fields, where the system is completely polarized, and the remaining inter-dot charge fluctuations are described by the SU(2) Kondo model subjected to the energy difference E [22, 23, 24]. The results obtained in both cases are shown in FIG. 6. In contrast to the magnetic field dependence discussed above, the conductance decreases monotonically as a function of E . The decrease is caused by the suppression of the inter-dot Kondo effect in the presence of finite energy difference E .

We note here that the ordinary "spin" Kondo effect still persists even in finite E , giving rise to the enhanced spin fluctuations. Although such enhancement in spin fluctuations may not be observed in transport properties, it should show up if we observe the NMR relaxation rate in the double-dot system. For example, the E -dependence of the NMR relaxation rate is exactly given by the function shown in FIG. 4: for large E , it is enhanced as $(E)^2$.

IV. TRIPLE-DOT SYSTEM

We now discuss how the above method can be used to calculate the conductance for multiple-dot systems with more than two dots. Here, we deal with a triple-dot system, and then briefly outline how to extend the method to N -dot systems. We will see that the conductance exhibits some characteristic properties under the control of the gate voltage and the magnetic field.

Let us consider a triple-dot system, for which three dots and three leads as arranged as shown in FIG. 7. Inter-dot tunneling t (intra- and inter-dot Coulomb repulsions) is assumed to be sufficiently small (large) here again. Therefore, one of the three dots can accommodate an electron thanks to strong intra- and inter-dot correlations. We focus on the Kondo regime, where the energy levels in the dots are sufficiently lower than the Fermi

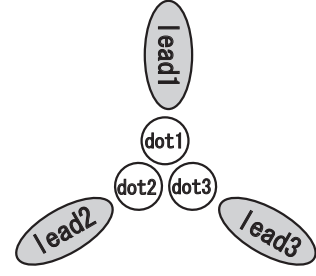


FIG. 7: Schematics of our triple-dot system: three dots are connected via small tunneling t , and each dot is connected to a lead via tunneling V . Inter- as well as intra-dot Coulomb repulsions are assumed to be sufficiently strong.

level. We note that a similar but different triple-dot system has been proposed recently [31] and its symmetry properties have been discussed.

In the second order in tunneling t , we can calculate the conductance between two leads in the triple-dot system by the exact solution of the SU(6) Anderson model, because there are 6 available electron states including spin degrees of freedom in the three dots. In this case, we can still utilize the formula Eq.(5) to calculate the conductance, where the strong inter-dot correlations among three dots are incorporated via the inter-dot susceptibility χ_{ops} between two dots through which electric currents flow.

A. gate-voltage control

Transport properties for the above three-dot systems depend on how the current is observed. To be specific, we change the gate voltage attached to the dot 3 with keeping the voltage in the dots 1 and 2 fixed, and observe the conductance between the leads 1 and 2 as well as between the leads 1 and 3.

The computed conductance is shown in FIG. 8(a) as a function of the energy difference E between the energy level in the dot 3 and those in the dots 1 and 2. We set the sign of E positive when the energy level in the dot 3 is higher than the others.

Let us first observe the current between the leads 1 and 2. It is seen that the conductance increases with the increase of E (> 0). This increase is attributed to the enhancement of the inter-dot Kondo effect in the presence of the energy difference, which is similar to that for the double dots in magnetic fields discussed in the previous section. At $E = 0$, the current flows via an SU(6) Kondo resonance (i.e. 6-fold degenerate Kondo resonance). On the other hand, for large E , the SU(4) Kondo effect is realized within 4 lower states in the dots 1 and 2. This gives the enhancement of the inter-dot susceptibility between the dots 1 and 2, resulting in the increase of the conductance. According to the exact solution of the SU(6) Anderson model [32], the effective

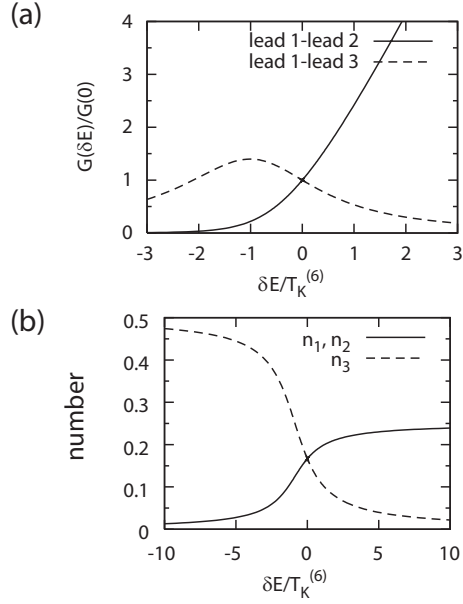


FIG . 8: (a)Conductance as a function of the energy difference. Here, $T_K^{(6)}$ is the Kondo temperature for SU (6) triple-dot system s. (b)the number of electrons for the asymmetric triple-dot as a function of the energy difference. The solid line is the number of electrons in the dot 1 or the dot 2 per spin and the dashed line is that in the dot 3.

Kondo temperature for large E is given by,

$$T_K^{(eff)}(E) = T_K^{(6)} \quad (E = T_K^{(6)})^{-1/2}; \quad (17)$$

and the corresponding conductance is

$$G(E = T_K^{(6)}) = T_K^{(6)}; \quad (18)$$

where $T_K^{(6)} = T_K^{(eff)}(E = 0)$ is the Kondo temperature for SU (6) triple-dot system s.

On the other hand, for $E < 0$, the SU (2) spin Kondo effect occurs in the lower 2 levels in the dot 3, while the spin Kondo effects in the dots 1 and 2 are suppressed because the number of electrons in the dots 1 and 2 decreases (see FIG . 8 (b)). Also, the inter-dot Kondo effect between the dots 1 and 2 is suppressed. As a result the conductance decreases when the current is observed between leads 1 and 2.

If the current is observed between the leads 1 and 3, distinct properties appear in the conductance. As seen from FIG . 8 (a), for large $|E|$ (irrespective of its sign), the conductance decreases because the energy difference suppresses the inter-dot Kondo effect between the dots 1 and 2. Notice that around $E = T_K^{(6)}$, the conductance has a maximum structure, where charge fluctuations between the dots 1 and 3 are slightly enhanced. Anyway, the conductance exhibits behavior similar to that observed in the double-dot case under the gate-voltage control.

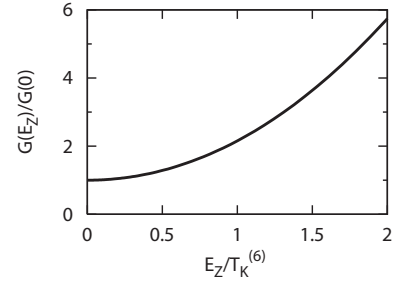


FIG . 9: Conductance as a function of the Zeeman splitting.

B. magnetic-field control

Let us now discuss how a magnetic field affects transport properties. For simplicity, we assume that the energy levels of three dots are same (symmetric dots). The computed conductance between two leads under magnetic fields is shown in FIG . 9. The conductance increases as the Zeeman splitting E_Z increases although the Kondo effect due to spin fluctuations are suppressed by the field. As discussed in the previous section, this enhancement is caused by the inter-dot Kondo effect among three dots. For large magnetic fields, half of the internal degrees of freedom are quenched, so that the symmetry of the system changes from SU (6) to SU (3). As a result, the SU (3) Kondo effect caused by inter-dot charge fluctuations is enhanced, and therefore the conductance is increased. The effective Kondo temperature in large fields is given as,

$$T_K^{(eff)}(E_Z) = T_K^{(6)} \quad (E_Z = T_K^{(6)})^{-1}; \quad (19)$$

and thus the conductance is enhanced like

$$G(E_Z = T_K^{(6)})^2; \quad (20)$$

C. generalization to system with more dots

We can generalize our method to systems with more than three dots: a lead is attached to each dot, where the electrons feel strong intra- and inter-dot Coulomb repulsions. All the dots are connected to each other via small inter-dot coupling t .

In similar manners mentioned above, we can calculate the conductance in such multiple-dot systems. The calculation can be done by using the formula Eq.(5) in the second order in tunneling t , where all the correlation effects are incorporated through the dynamical susceptibility. We can use the exact solution of the SU (2N) Anderson model [25] for an N-dot system. The conductance shows similar properties to those observed in the double and triple dots: if we change the gate voltage of the dot, the conductance between the lead and one of the other leads is generally suppressed, while it is enhanced otherwise.

In this paper we have assumed small inter-dot coupling t , and calculated the conductance up to t^2 . It should be mentioned that for a system with more than two dots, a Fano-type interference effect may emerge in higher order terms in t . This interference effect may give another interesting aspect of multiple-dot systems, which is to be studied in the future work.

V. SUMMARY

We have studied transport properties in the double-dot system connected in series that possesses not only intra-but also inter-dot Coulomb repulsions. It has been shown that the application of the Ward-Takahashi identity enables us to use the exact solutions of the Anderson model for calculations of the conductance at zero temperature. We have clarified how the inter-dot Kondo effect affects the conductance under the gate-voltage control and the magnetic field control. In particular, the conductance is decreased by the suppression of the inter-dot Kondo effect in the gate-voltage control, whereas it is increased by the enhanced Kondo effect in the presence of magnetic fields. The latter conclusion is consistent with the results of the numerical renormalization group. The method has also been applied to calculate the conductance in multiple-dot systems including more than two dots. By taking a triple-dot system as an example, we have shown how the conductance is controlled by tuning the inter-dot Kondo effect.

Naively, it seems not easy to observe the Kondo effect in multiple-dot systems (more than two dots) experimentally. We would like to mention, however, that the Kondo temperature in multiple-dot systems can be much higher than that in single-dot systems when the inter-dot repulsion is relevant, as assumed in this paper. Therefore, if

such multiple-dot system could be fabricated, the Kondo effect may be possibly observed even in multiple-dot systems considered here.

Finally a comment is in order on the ordinary "spin" Kondo effect in our multiple-dot system. We have focused on the inter-dot "orbital" Kondo effect in this paper, which directly affects transport properties. Concerning the spin Kondo effect, the impacts of the gate voltage and the magnetic field appear differently from the inter-dot Kondo effect, e.g. the magnetic field (gate-voltage difference) suppresses (enhances) the spin Kondo effect. If we use the dynamical spin susceptibility instead of the pseudo-spin susceptibility, the present analysis can be straightforwardly applied to low-frequency dynamics such as the NMR relaxation rate, which may be important to discuss an application to quantum bits in quantum computation. In fact, the expression Eq.(8) gives the NMR relaxation rate for the double-dot system, if the dynamical susceptibility is regarded as the spin susceptibility. It is of particular interest that the NMR relaxation rate in our multiple-dot systems can be controlled by the gate voltage, e.g. the difference in the energy-levels of double dots can enhance the relaxation rate.

After the completion of this paper, we became aware of a recent preprint which deals with the SU(4) Kondo effect in a slightly different model [33].

Acknowledgments

We would like to express our sincere thanks to M. Eto for valuable discussions. R.S. also thanks H. Akai for fruitful discussions and supports.

-
- [1] L. P. Kouwenhoven, D. G. Austing and S. Tarucha, *Rep. Prog. Phys.* **64**, 701 (2001)
 - [2] S. M. Reimann, *Rev. Mod. Phys.* **74**, 1283 (2002)
 - [3] T. K. Ng and P. A. Lee, *Phys. Rev. Lett.* **61**, 1768 (1988)
 - [4] L. I. Glazman and M. E. Raikh, *JETP Lett.* **47**, 452 (1988)
 - [5] A. Kawabata, *J. Phys. Soc. Jpn.* **60**, 3222 (1991)
 - [6] W. Izumida, O. Sakai and Y. Shimizu, *J. Phys. Soc. Jpn.* **67**, 2444 (1998)
 - [7] W. Hofstetter, J. König and H. Schoeller, *Phys. Rev. Lett.* **87**, 156803 (2001)
 - [8] M. Eto and Y. V. Nazarov, *Phys. Rev. B* **64**, 085322 (2001)
 - [9] A. Oguri, *J. Phys. Chem. Solids* **63**, 1591-1594 (2002); *Phys. Rev. B* **64**, 153305 (2001)
 - [10] D. Goldhaber-Gordon, H. Shtrikman, D. Mahalu, D. Abusch-Magder, U. Meirav and M. A. Kastner, *Nature (London)* **391**, 156 (1998); S. M. Cronenwett, T. H. Oosterkamp, L. P. Kouwenhoven, *Science* **281**, 540 (1998); J. Schmid, J. Weis, K. Eberl and K. v. Klitzing: *Physica B* **256**, 182 (1998)
 - [11] S. Sasaki, S. De Franceschi, J. M. Elzerman, W. G. van der Wiel, M. Eto, S. Tarucha and L. P. Kouwenhoven, *Nature*, **405**, 764 (2000)
 - [12] S. Y. Cho, H. Q. Zhou and R. H. McKenzie, *Phys. Rev. B* **68**, 125327 (2003)
 - [13] S. Nagatsuma, J. P. Leburton and R. M. Martin, *Phys. Rev. B* **60**, 8759 (1999)
 - [14] W. G. van der Wiel, S. De Franceschi, J. M. Elzerman, T. Fujisawa, S. Tarucha and L. P. Kouwenhoven, *Rev. Mod. Phys.* **75**, 1 (2003)
 - [15] Daniel S. Saraga and Daniel Loss, *Phys. Rev. Lett.* **90**, 166803 (2003)
 - [16] T. Aono, M. Eto and K. Kawamura, *J. Phys. Soc. Jpn.* **67**, 1860 (1998)
 - [17] A. Georges and Y. Meir, *Phys. Rev. Lett.* **82**, 3508 (1999)
 - [18] H. Joeng, A. M. Chang and M. R. Melloch, *Science* **293**, 2221 (2001)
 - [19] K. Kikoin and Y. Avishai, *Phys. Rev. Lett.* **86**, 2090 (2001); *Phys. Rev. B* **65**, 115329 (2002); Y. Takazawa,

- Y. Imai, and N. Kawakami, J. Phys. Soc. Jpn. 71, 2234 (2002).
- [20] Y. Tanaka and N. Kawakami, J. Phys. Soc. Jpn. 73, 2795 (2004).
- [21] G. B. Martins, C. A. Busser, K. A. Al-Hassanieh, A. Moreo and E. Dagotto, Phys. Rev. Lett. 94, 026804 (2005)
- [22] U. Wilhelm and J. Weis, Physica E 6, 668 (2000)
- [23] Q. F. Sun and H. Guo, Phys. Rev. B 66, 155308 (2002)
- [24] L. Borda, G. Zarand, W. Hofstetter, B. I. Halperin, and J. von Delft, Phys. Rev. Lett. 90, 26602 (2003)
- [25] P. Schlottmann, Phys. Rev. Lett. 50, 1697 (1983); N. Kawakami and A. Okiji, J. Phys. Soc. Jpn. 54, 685 (1985)
- [26] H. Shiba, Prog. Theor. Phys. 54 967 (1975)
- [27] A. Nakamura, N. Kawakami and A. Okiji, J. Phys. Soc. Jpn. 56, 3667 (1987); R. Sakano and N. Kawakami, to be published in Proceedings of International Symposium on the Creation of Novel Nanomaterials, Journal of Electron Microscopy, Supplement (2005)
- [28] F. D. M. Haldane, Phys. Rev. Lett. 40, 416 (1978); J. Phys. C 11, 5015 (1978)
- [29] S. Sasaki, S. Amano, N. Asakawa, M. Eto and S. Tanucha, Phys. Rev. Lett. 93, 017205 (2004); M. Eto, J. Phys. Soc. Jpn. 74, 95 (2004)
- [30] O. Yu. Kolesnychenko, R. de Kort, M. I. Katsnelson, A. I. Lichtenstein and H. Van Kempen, Nature (London) 415, 507 (2002); A. K. Zhuravlev, V. Yu. Irkhin, M. I. Katsnelson and A. I. Lichtenstein, Phys. Rev. Lett. 93, 236403 (2004)
- [31] T. Kuzmenko, K. Kikoin and Y. Abishai, cond-mat/0412527; see also, Phys. Rev. Lett. 89, 156602 (2002)
- [32] P. Schlottmann, Phys. Rev. B 30, 1454 (1984)
- [33] A. L. Chudnovskiy, preprint, cond-mat/0502282